Journal of Chromatography, 631 (1993) 133–144
Elsevier Science Publishers B.V., Amsterdam

CHROMSYMP. 2598

Axial illumination of fused-silica capillaries

Investigation of fluorescence and refractive index detection

Ahmad A. Abbas and Dennis C. Shelly

Department of Chemistry and Biochemistry, Texas Tech University, Lubbock, TX 79409 (USA)

ABSTRACT

The optical waveguide properties of fused-silica capillaries enable greater illuminated sample volume by axial illumination, as compared to cross capillary illumination. Several modes of light propagation inside these unique optical waveguides are described. A micro-LC flow cell featuring axial illumination with mobile phase elimination by nebulization has been developed and evaluated. This device was used in the construction and evaluation of laser-induced fluorescence and laser-based refractive index detectors. A summary of results from our studies and a survey of the various detection possibilities, theoretically compatible with axial illumination of capillary waveguides, are presented.

INTRODUCTION

While small-dimensional capillaries (10–250 μm inner diameter) provide high-efficiency separations, these capillaries generate extremely small path lengths when cross-capillary illumination is employed. This results in very small probed volumes, hence very small analytical signals, complicating detection by photometric means. This problem can be largely overcome by axial illumination. Here, the entire sample band can be illuminated generating significantly higher detection efficiency.

Axial illumination of fused-silica capillaries has recently been utilized as a technique for increasing detection capabilities in capillary separations. Significant increases in concentration sensitivities of absorption and fluorescence detection, due to the increased optical path length achievable with axial illumination, have been shown. Grant and Steuer [1] first reported on an "extended path length" UV absorbance detector for capillary electrophoresis in 1990. The measurement was based on indirect fluorescence which was spatially modulated by fluorophore displacement. Xi and Yeung [2] demonstrated enhanced performance for absorption detection in open tubular capillary liquid chromatography. A 1000-fold increase in pathlength was observed. Further, it was noted that the entire sample band could be illuminated, thus confining the detection region to the chromatographic band. Even with the very low flow-rates of open tubular capillary liquid chromatography, optical distortions were observed as light was coupled into the capillary flow cell. Taylor and Yeung [3] described an axial-beam absorbance detector for capillary electrophoresis that was used to monitor the separation of bromothymol blue and bromocresol green. A red helium–neon laser was used for excitation. A conventional light source (actually a commercially available UV–Vis absorption detector) and axial illumination has also been used

Correspondence to: D. C. Shelly, Department of Chemistry and Biochemistry, Texas Tech University, Lubbock, TX 79409, USA.

0021-9673/93/$06.00

for absorbance detection in capillary electrophoresis [4]. Fluorescence detection in capillary zone electrophoresis, via axial illumination, has been reported by Sweedler *et al.* [5]. Axial illumination combined with the unique scanning capabilities of a charge coupled device detector resulted in concentration detection limits between $2 \cdot 10^{-20}$ and $8 \cdot 10^{-20}$ mol for fluorescein isothiocyanate–amino acids conjugates.

Despite these recent reports of axial illumination detection in open tubular capillary liquid chromatography and capillary electrophoresis, to date, no effort has been documented for the coupling of axial illumination with slurry packed capillary LC (micro-LC) [6]. The major impediment to this instrumental achievement is solvent elimination with minimal optical distortion in this higher mobile phase flow-rate separation technique [7]. Flow-rates of 1 to 3 μl/min result in significant difficulty in effectively coupling light into the exit capillary (waveguide). The liquid droplet acts as a lens, defocusing the beam and modulating the light energy distribution in the capillary. The mobile phase must be eliminated from the waveguide orifice to prevent distortions of optical coupling.

This paper described our attempts in coupling axial illumination with micro-LC. A unique, nebulizing flow cell was designed and fabricated. The operating chracteristics of this flow cell and the detection performance of a laser-induced fluorescence instrument and a laser-based refractive index detector are presented.

THEORY

Axial illumination of long capillary cells has been fairly extensively studied. Lei *et al.* [8] used 50-m capillary cell for colorimetry. Improvement in absorbance of between 130 and 300 was reported for carbon disulfide solutions of phosphomolybdenum heteropoly blue. Dasgupta [9] reported wide dynamic range and high sensitivity using a reflective helical cell. A decreasing non-linear dependance of effective pathlength with increasing solution absorbance was noted. Tsunoda *et al.* [10] have analyzed the optical transmission characteristics of long capillary cells where total internal reflection occurred at the outer wall surface. A borosilicate glass capillary showed better transmission than one with mirrored

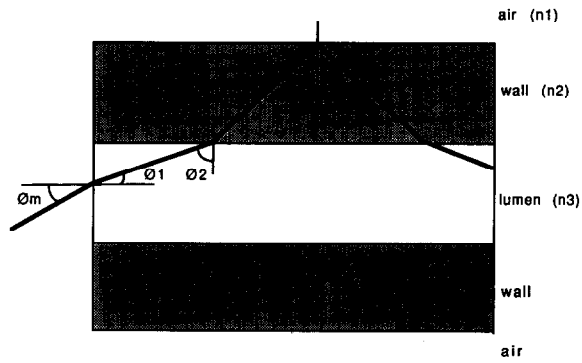

Fig. 1. Ray diagram for light propagation in a capillary waveguide. n_1, n_2 and n_3 are the refractive indices of air, wall and lumen, respectively. $\emptyset_2$ and $\emptyset_3$ are the angles subtended by light at the lumen-wall and wall-air interfaces, respectively. $\emptyset_m$ is half the acceptance angle.

walls. The importance of wall refractive index was noted which contributed to a subsequent paper describing the use of poly(tetrafluoroethylene co-hexafluoropropylene) tubing (refractive index was almost identical to water) for such cells [11]. Since a detailed analysis of light transmission in fused-silica capillaries is somewhat redundant and beyond the scope of this paper, we present a brief treatment of this topic, showing the relationship of mobile phase refractive index and effective optical pathlength in an axially illuminated capillary column/flow cell.

When light is launched axially in the lumen of a circular fused-silica capillary, all light energy can be trapped inside the capillary if total internal reflection at the wall/air interface occurs as shown in Fig. 1. This is possible only if inequality 1, based on Snell's law, is satisfied.

$$\sin \emptyset_2 > n_1/n_3 \quad (1)$$

The light energy distribution inside these capillary optical waveguides can be classified into three pathways: (a) light energy distributed only in the wall of the capillary; (b) light energy distributed only in the lumen; and (c) light energy distributed in the wall *and* the lumen of the fused-silica capillary. These three pathways are illustrated in Fig. 2, using a classical ray diagram approach. Pathways b and c, where light energy transmits across the medium inside the lumen, is of prime importance when mak-

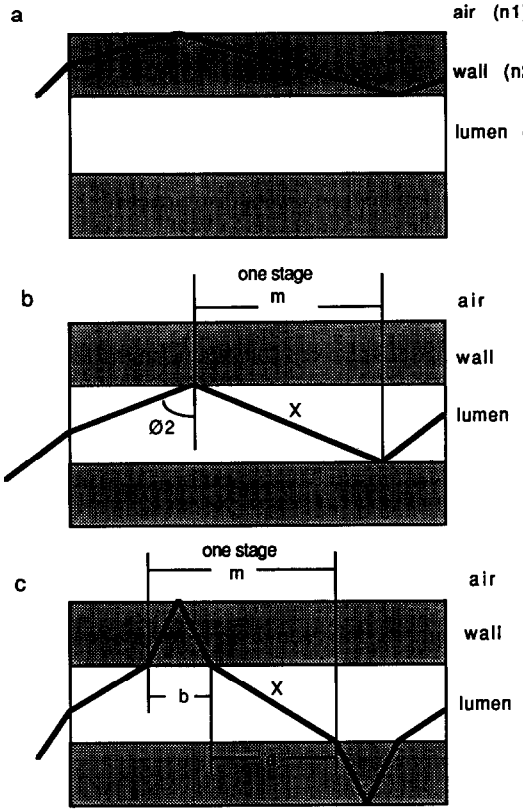

Fig. 2. Light propagation pathways in capillary waveguides. (a) Wall propagation; (b) lumen propagation; (c) combination propagation. $Ø_2$ is any angle from the critical angle to 90°. m, X, a and b are distances, as shown.

ing absorbance, fluorescence or refractive index measurements.

Most of light energy will be distributed in pathway b if

$$n_2 < n_3 \sin Ø_2 \quad (2)$$

where $Ø_2$ is the range of angles from the critical angle to 90°. Here, $n_2 < n_3$, the refractive index of fused silica ($n_2 = 1.458$) is less than that of the mobile phase. If $n_2 > n_3$ then light will traverse according to pathway c. It should be clear that most hydroorganic mobile phases will result in either pathways b or c. Pathway a explicitly occurs only when light is launched into the capillary wall.

Only radiation which traverses the lumen will significantly interact with chromatographic analytes. The effective pathlength (l_e), defined as the total distance travelled by light in the lumen, is an indication of the light energy distribution inside a capillary optical waveguide. l_e is the product of the distance that light travels in the lumen for one "stage" (see ref. 11) and the number of "stages". We have chosen an optical window of 0.9 cm, which is the diameter of our photomultiplier tube. For pathway b, l_e is calculated using eqn. 3.

$$l_e = nX = l_p/\sin Ø_2 \quad (3)$$

where X is the distance that light travels in the lumen in one stage (see Fig. 2). l_p is the physical cell length, which depends on the imaged detector diameter. For pathway c, l_e is calculated using eqn. 4.

$$l_e = l_p\, X/(A+B) \quad (4)$$

where A is the ratio of $(d_c n_1)$ to $(\cos Ø_2 n_3)$ and B is the ratio of $(2d_w n_1)$ to $(\cos Ø_3 n_2)$. $Ø_3$ is shown in Fig. 1. d_c and d_w are the lumen and wall thicknesses, respectively. The derivation of eqns. 3 and 4 and the detailed interpretation of them are the subject of a future paper.

The dependence of l_e on mobile phase refractive index is illustrated in Fig. 3. Since n_1 and n_2 are fixed, l_e varies with n_3 for each pathway, as shown. For pathway b, effective pathlength varies linearly with lumen refractive index ($n_2 < n_3$), while for pathway c, effective pathlength varies non-linearly with lumen refractive index ($n_2 > n_3$). Note the dis-

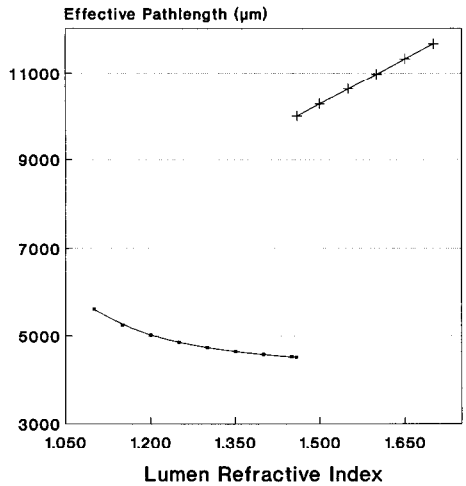

Fig. 3. Variation of effective pathlength with lumen refractive index. (□) $n_2 > n_3$; (+) $n_2 < n_3$.

continuity in the plot. This occurs at the refractive index of fused silica, 1.458, where propagation pathway c sharply changes to pathway b. The relative magnitudes of l_e approximate those of a solute band. These effective pathlengths correspond to illuminated volumes of 100 to 500 nl, typically found in micro-LC.

The variation of light energy distribution with lumen refractive index is, in fact, more complicated than that described above. For both pathways the acceptance angle (the solid angle through which light is gathered into propagating modes in the waveguide) changes with n_3, the lumen refractive index. For pathway b, the acceptance angle increases from 9 to 25° when n_3 goes from 1.468 to 1.510. For pathway c, the acceptance angle increases from 27 to more than 90° when n_3 extends from 1.359 to 1.432. Thus, in pathway c much more light is coupled into the capillary than for pathway b. Remembering that typical mobile phase refractive indices are less than that of fused silica, pathway c represents the situation for axial illumination detection in most chromatographic applications. Even though l_e decreases as the mobile phase refractive index approaches that for fused silica, for pathway c, the light gathering power increases tremendously, allowing more light to couple into the cell, resulting in greater light energy distribution in the lumen. This issue with also be treated in a separate, more detailed publication.

By examining the above ray diagrams and plots it should be clear that axial illumination affords several types of detection modes. If incident light is not absorbed by analyte, propagating light may be coupled out of the capillary for a measurement of lumen refractive index. If exciting light is absorbed, is not reemitted as fluorescence, and is coupled out of the capillary a measurement of absorbance is accomplished. Fluorescence is also measureable if this emitted light can be detected. The unique feature of these possibilities is the manner in which the analytical signal is detected, *i.e.* how the light is coupled out of the capillary. We show, in this paper, the measurement of refractive index and fluorescence. Absorbance measurements have already been reported by Xi and Yeung [2].

EXPERIMENTAL

Axial illumination micro-LC flow cell

The key component of our detection systems is a flow cell that permits axial illumination with simultaneous mobile phase elimination by nebulization. Fig. 4 shows a drawing of the key features of this cell. Nebulization is based on the Babington principle (see ref. 12). The capillary orifice is carefully positioned over the gas outlet as shown. The gas jet is formed by the conical-shaped polyurethane film that is compressed between the plastic manifold and the metal plate. The capillary (Polymicro Technologies, Phoenix, AZ, USA), which has been stripped of its polyimide, is held against the plastic gas manifold with a glass plate. This assembly is positioned against a modified mirror mount (Newport Corp., Fountain Valley, CA, USA) with an aluminum clamp, as shown in Fig. 5. A spray barrier prevents contamination of optics. Using 100 p.s.i. (1 p.s.i. = 6894.76 Pa) air, mobile phase flow-rates approaching 10 μl/min can be nebulized with this cell. Neither the flow cell nor the nebulizing gas are heated.

Laser-induced fluorescence apparatus

The laser-induced fluorescence apparatus was similar to that described previously [13]. The instrument consisted of a Model 4220N (442 nm) helium–cadmium laser and a Model 3315I (325 nm) helium–cadmium laser (Liconix, Santa Clara, CA, USA), a miniature photon-counting detector [14] and suitable optics, as illustrated in Fig. 6. A quartz, f/1.5 plano convex lens (Oriel, Stratford, CT, USA) was used to focus the 325-nm laser beam onto the capillary orifice. A 10 × microscope objective performed this function for the 442-nm laser. Fluorescent light was collected through the large opening, orthogonal to the capillary flow/excitation optical axis using an integrally-mounted cylindrical lens (f/1.5, Melles Griot, Irvine, CA, USA). The sampling rate for the data system was based on a counting gate time of 64 ms.

Refractive index apparatus

The refractive index detection apparatus consisted of the Micro LC flow cell, in somewhat modified form, and a helium–neon laser (Melles Griot, Irvine, CA, USA). The refractive index flow cell is shown in Fig. 7. Here, an optical fiber (200 μm core

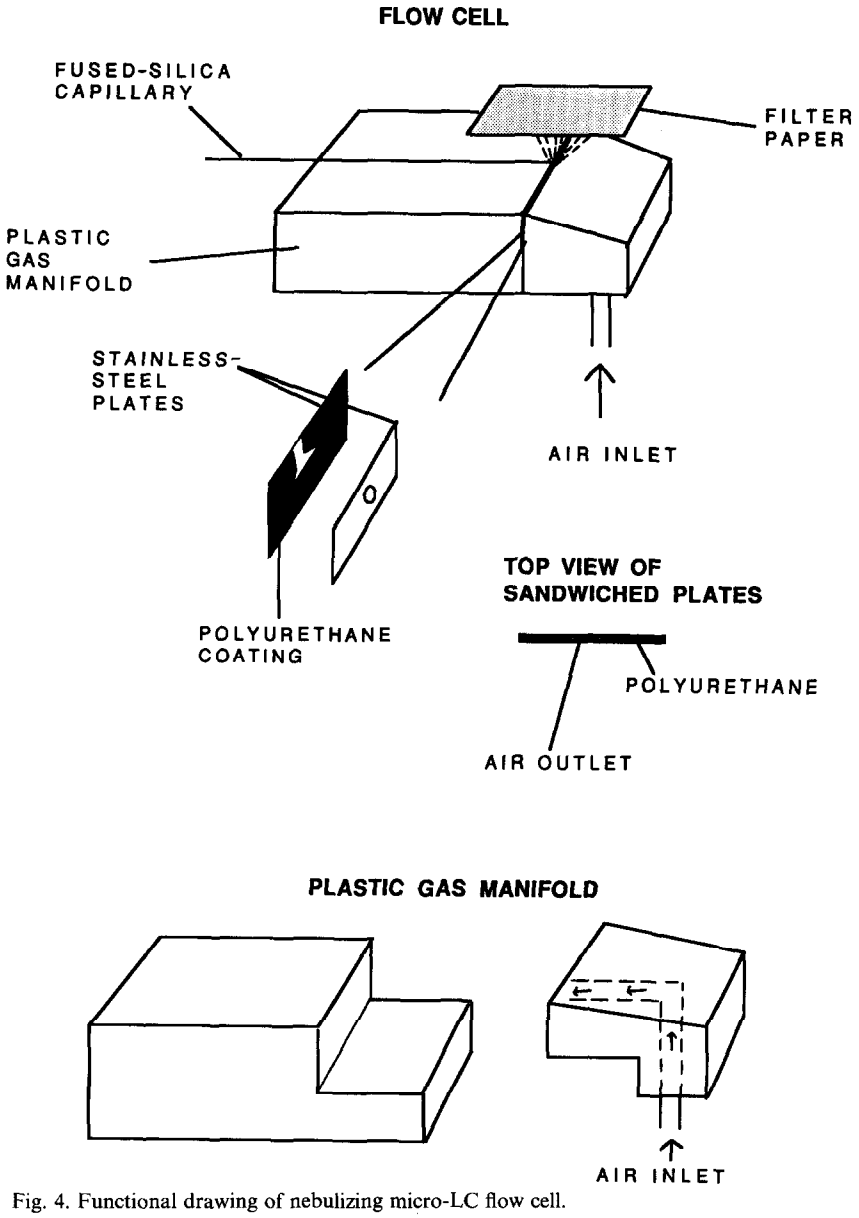

Fig. 4. Functional drawing of nebulizing micro-LC flow cell.

diameter, Polymicro Technologies) was optically coupled to the flow cell capillary using an optical coupling gel (General Fiber, Cedar Grove, NJ, USA). The distance between the contact/coupling point and the capillary orifice was about 2 cm. As shown in Fig. 8, a beam splitter (microscope slide) directed a portion of the helium neon laser beam to a reference fiber. A 10× microscope objective focused the laser beam onto the capillary orifice. The sample and reference fibers were optically coupled with miniature photocell detectors (S2007; Electronic Goldmine, Scottsdale, AZ, USA). The output from each photocell was electronically connected to a log ratio amplifier (AD757N; Analog De-

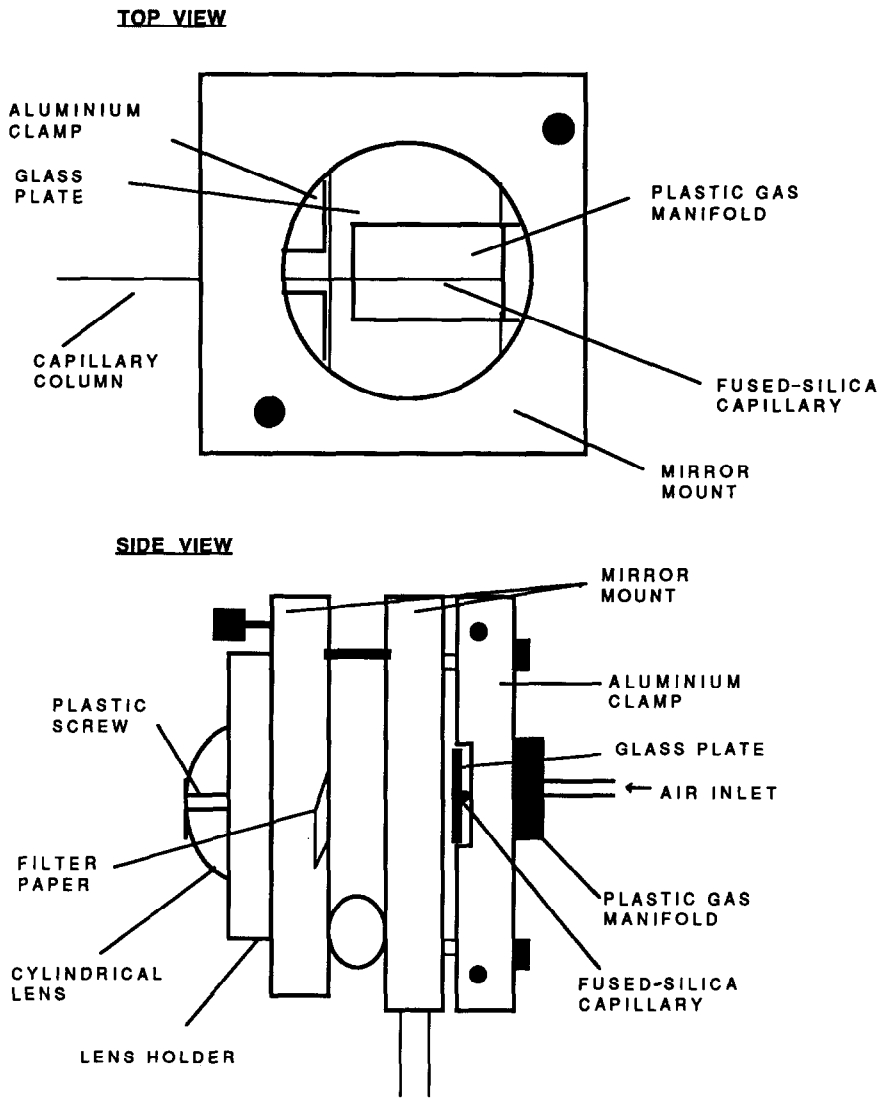

Fig. 5. Schematic diagram of fluorescence flow cell.

vices, Norwood, MA, USA). Analog output was recorded on a standard, laboratory strip chart recorder.

Micro liquid chromatography

Our micro-LC system consisted of a Model 8500 syringe pump (Varian, Walnut Creek, CA, USA) and a C14W microinjector (Valco, Houston, TX, USA) that was equipped with a 100-nl internal loop. All injections were of the moving loop type [15]. 250 μm inner diameter fused-silica capillaries (Polymicro Technologies) were packed with a computer-controlled pump [16]. Dynamic measurements of perylene were based on a reversed-phase separation, for which Spherisorb ODS2 (5 μm) packing was used. For aflatoxin chromatography LiChrosorb SiOH (10 μm diameter) particles were used to pack the column. All packings were obtained from Alltech (Deerfield, IL, USA) and both micro-LC columns were 70 cm long.

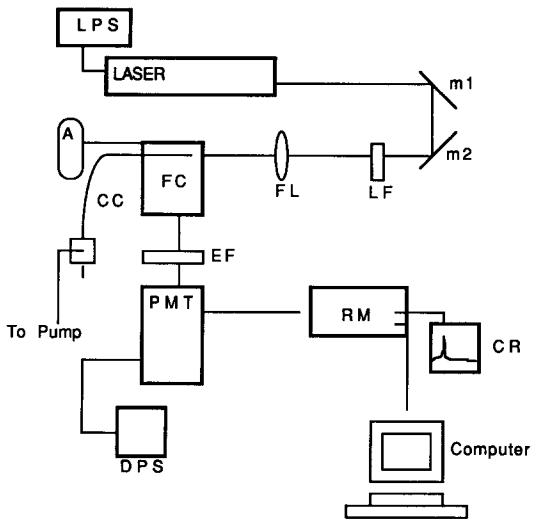

Fig. 6. Schematic of fluorescence apparatus. LPS = Laser power supply; m1, m2 = first surface mirrors; LF = liquid filter; FL = focusing lens; FC = flow cell; CC = chromatographic column; A = air supply; I = microinjector; EF = emission filter; PMT = photomultiplier tube; DPS = detector power supply; RM = ratemeter; CR = chart recorder.

Chromatogram and data analysis

All fluorescence chromatograms were analyzed with DADiSP (DSP Development Corp., Cambridge, MA, USA), digital signal processing software. Various operations, such as signal acquisition of baseline and peaks, peak integration, width at half height, etc., were easily performed with this system.

Chemicals and reagents

All mobile phase reagents were "HPLC" grade or "reagent" grade and were used without further purification. Purified water was obtained from a Nanopure treatment system (Sybron/Barnstead, Boston, MA, USA). All chromatographic solutes were "reagent" grade and were not further purified prior to use. The aflatoxins were purchased as a kit, AF-1, from Sigma (St. Louis, MO, USA).

RESULTS AND DISCUSSION

Flow cell set-up and operation

The successful operation of our flow cell depended entirely on how well the liquid droplet was eliminated at the outlet orifice of the capillary. For efficient nebulization it was important to have the dimensions of the nebulizer as small as possible. The jet orifice dimensions were 50 μm width and 500 μm length. Optimum placement of the capillary relative to the jet orifice was necessary for continuous and stable nebulization. It has been reported that vibrations of the capillary produced tremendous optical distortions [2] with axial illumination. In our design a glass plate was placed over the capillary cell and clamped into position, thus eliminating vibrations and microbending losses. Tremendous baseline fluctuations (optical distortions) resulted when either inefficient nebulization or an incompletely fixed capillary occurred. The design of our flow cell made it convenient to work with stripped fused-silica capillaries, even though removal of the polyimide coating gave a fragile capillary flow cell. Another important factor was that extreme cleanliness of the excitation and emission optics was necessary to maintain the highest possible sign-to-noise ratio. Our nebulizing flow cell was effective in nebulizing all mobile phases tested, which included 100% methanol, 100% ethanol, benzyl alcohol–ethanol, acetonitrile–water and toluene–ethylacetate–methanol–formic acid mixtures.

Laser-induced fluorescence measurements

To evaluate our flow cell design we performed a series of experiments using perylene solutions of different concentrations. Static and dynamic measurements of perylene were made, using solutions ranging from $1.34 \cdot 10^{-9}$ to $1.34 \cdot 10^{-6}$ M and $1.31 \cdot 10^{-8}$ to $1.31 \cdot 10^{-5}$ M, respectively. Normal-phase micro-LC of aflatoxins was performed in order to determine the practical limits of detection.

Static evaluation

Using a syringe pump (Harvard Apparatus, Dover, MA, USA), perylene solutions of different concentrations were pumped, at a flow-rate of 5 μl/min, through the optical window (stripped fused-silica capillary flow cell), whose dimensions were: inner diameter 99 μm, length 0.9 cm, volume 69.2 nl. Fluorescence was recorded over a 20–30-min period for each solution. Laser power (442 nm) at the flow cell entrance was approximately 1.5 mW.

As shown in Table I, four different concentrations of perylene were prepared in each of four sol-

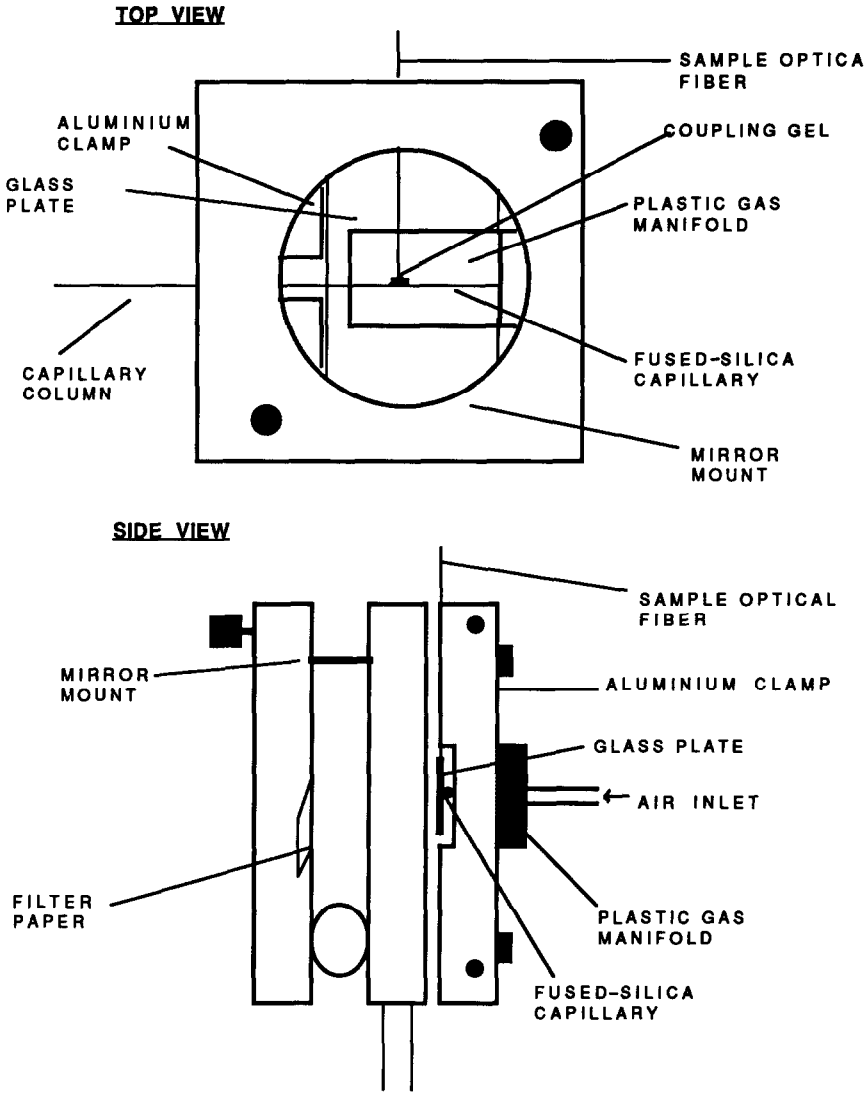

Fig. 7. Drawing of refractive index flow cell.

vents, containing various proportions of ethanol (n = 1.359) and benzyl alcohol (n = 1.54) in order to achieve different refractive index values. Two solutions had refractive indices lower than fused silica and two solutions had higher refractive indices than fused silica. Table I shows the mean photon counts, after subtracting the blank (photon counts for solution without perylene), obtained for the sixteen solutions. The blank spaces for 10^{-6} M and 10^{-9} M solutions are explained by the fact that 10^{-9} M solutions (refractive index lower than that of fused silica) were too weak to be detected and the signal for 10^{-6} M solutions (refractive index greater than that of fused silica) was so high that it saturated the PMT photocathode!

Fig. 9 shows a series of signal *versus* concentrations plots of the 4 datasets listed in Table I. The slopes (sensitivities) are given in the caption. Notice that sensitivities increase with lumen refractive index. The large difference in the slope values for so-

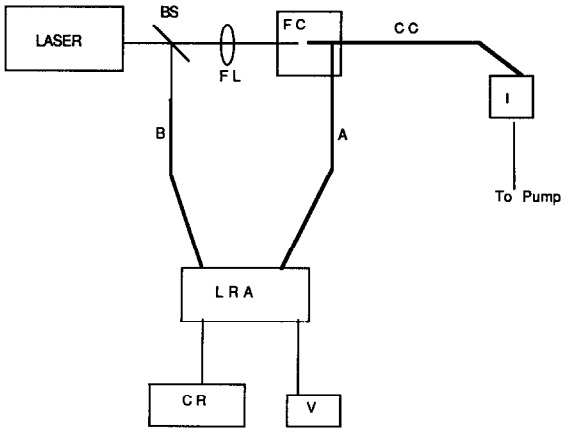

Fig. 8. Schematic of refractive index apparatus. BS = Beam splitter; FL = focusing lens; FC = flow cell; A = sample optical fiber; B = reference optical fiber; LRA = log ratio amplifier; CR = chart recorder; V = voltmeter; CC = chromatographic column; I = microinjector.

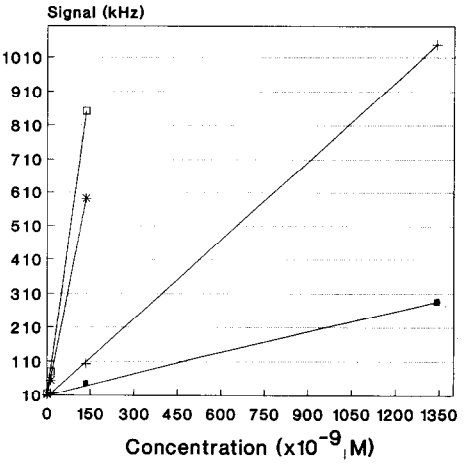

Fig. 9. Response plots, static perylene measurements. ■ = Ethanol, $n3$ = 1.359 (slope 0.204); + = ethanol–benzyl alcohol (3:2, v/v), $n3$ = 1.432 (slope 0.779); * = ethanol–benzyl alcohol (2:3, v/v), $n3$ = 1.468 (slope 4.40); □ = ethanol–benzyl alcohol (1:4, v/v), $n3$ = 1.510 (slope 6.34).

lutions which have refractive indices less than 1.458 compared to those solutions with refractive indices greater than 1.458 can be attributed to the fact that when the lumen refractive index is less than the refractive index of the fused-silica wall, pathway c (refer to Fig. 2) is the dominant mode of light propagation inside the flow cell. Therefore, light energy is distributed in *both* the wall and the lumen of the fused-silica capillary flow cell. When the refractive index of the lumen is higher than that of fused silica, pathway b (see Fig. 2) is the preferred mode of propagation. In this case, almost all light energy is trapped inside the lumen, resulting in higher slopes, hence greater detection sensitivities. More light-sample interaction occurs when lumen refractive index is close to and higher than that of the wall.

TABLE I

STATIC MEASUREMENTS OF PERYLENE

S1, S2, S3 and S4 are signal intensities for solutions of refractive index = 1.359, 1.432, 1.468 and 1.510, respectively.

Concentration (M)	S1	S2	S3	S4
$1.34 \cdot 10^{-9}$			10.4	15.4
$1.34 \cdot 10^{-8}$	11.6	15.4	54.2	78.8
$1.34 \cdot 10^{-7}$	46.1	103.3	590.6	851.8
$1.34 \cdot 10^{-6}$	286	1047.3		

Dynamic evaluation

In order to make dynamic measurements of perylene we connected the flow cell to a 70-cm long slurry-packed capillary column. An acetonitrile–water (96:4) mobile phase, with a refractive index of 1.344, was passed through the column at constant pressure (3000 p.s.i.), which corresponded to a flow-rate of about 5 μl/min. Perylene solutions, varying in concentration from $1.31 \cdot 10^{-8}$ to $1.31 \cdot 10^{-5}$ M, were injected onto the column using a 10-s moving loop technique. The volume injected was approximately 80 nl.

Perylene detection in the dynamic mode showed reasonable analytical figures of merit. The minimum detectable concentration and quantity (with signal-to-noise ratio 3) are calculated as $3.46 \cdot 10^{-10}$ M and $1.38 \cdot 10^{-14}$ g, respectively, using the procedure described by Scott [17]. The response index (linearity) was calculated as 0.486 over the range cited above, therefore the linear range was less than 4 orders of magnitude. These are not quite as good as we have achieved in the past [13] due, mostly, to very low laser power (1.5 mW) delivered

to the cell with the microscope objective. Other factors include low mobile phase refractive index and the small PMT photocathode area. Rationale, for the former is explained above. The influence of detector area is obvious when considering that less light, hence less illuminated volume, is detected with a small area photodetector.

Aflatoxin micro-LC

Aflatoxins are among the most potent carcinogens known [18]. Aflatoxins B1, B2, G1 and G2 are the commonly occurring aflatoxins in food products. Subpicogram levels of these aflatoxins have been quantitatively detected using high-pressure liquid chromatography in conjunction with laser-induced fluorescence [19]. The most potent of these aflatoxins, B1, is the least fluorescent and its detection at very low levels has been a challenge. It has been shown that the mobile phase plays an important role in fluorescence properties of these species. With mobile phases such as chloroform and dichloromethane G1 and G2 showed excellent fluorescence but emission from B1 and B2 was markedly quenched [20]. One paper reported that the use of a mobile phase mixture consisting of toluene–ethyl acetate–methanol–formic acid (89:7.5:1.5:2), gave the largest magnitude signals with the shortest overall separation time [21]. Any changes in this "optimum" ratio changed both the chromatographic and fluorescence properties of the analytes.

Since the refractive index of this unique mobile phase is very close to the refractive index of toluene (1.49), we found that it would be the most suitable for exploring the capabilities of fluorescence detection with axial illumination. A 150-μm capillary yielded a flow cell volume of 159 nl, length = 0.9 cm, and was used in the nebulizing flow cell for isocratic, normal-phase chromatography of aflatoxins B1, G1 and G2. Fig. 10 shows a typical chromatogram of the mixture, at injected concentrations $6.4 \cdot 10^{-6}$, $7.8 \cdot 10^{-6}$ and $6.4 \cdot 10^{-6}$ M, respectively. The inset shows the three components near their detection limits.

Prior to obtaining analytical figures of merit, we studied the effect of formic acid concentration on retention and detectability. When added in the proportions 0.3, 1 and 2% (v/v), we found that larger amounts of formic acid dramatically increased detection and decreased retention, especially at the 2% level (data not shown). Levels higher than 2% were not attempted due to imcompatibilities with the syringe pump.

Analytical figures of merit for the chromatogram of Fig. 10 are listed in Table II. These data show better concentration and mass detectability, compared to perylene. We attribute this to better laser focussing since the laser power at the entrance of the capillary flow cell was 6.5 mW, approximately 4 times greater than the laser power attained in the perylene measurements. Also, the aflatoxin mobile phase refractive index was higher than the perylene mobile phase, allowing more light to interact with the analytes in the aflatoxin detection.

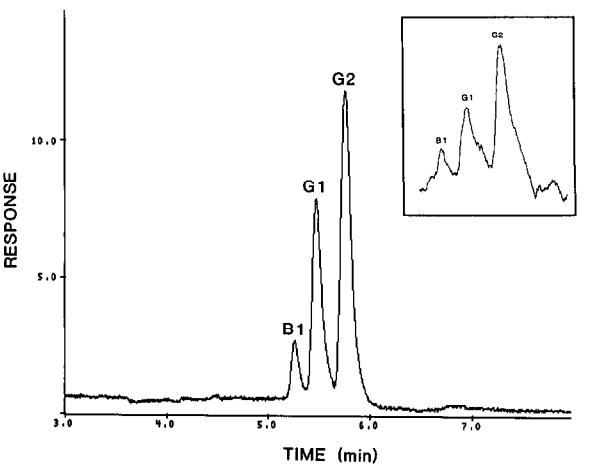

Fig. 10. Aflatoxin chromatogram. See text for details.

Refractive index measurements

Any light energy that propagates in the capillary wall can be coupled out of the tubular lightguide

TABLE II

ANALYTICAL FIGURES OF MERIT FOR AFLATOXINS

MDC = Minimum detectable concentration; MDQ = minimum detectable quantity.

	Aflatoxin		
	B1	G1	G2
MDC	$1.02 \cdot 10^{-9}$ M	$1.45 \cdot 10^{-10}$ M	$3.7 \cdot 10^{-11}$ M
MDQ	$5.05 \cdot 10^{-14}$ g	$7.56 \cdot 10^{-15}$ g	$1.94 \cdot 10^{-15}$ g

and detected. The amount of light that propagates in the wall will be strongly influenced by lumen refractive index, as seen in the Theory section. In this way, the axial illumination flow cell may be used for refractive index measurements, provided that the analyte does not absorb at the analytical wavelength. Several techniques have been used for coupling light from optical lightguides [22]. The simplest approach is to provide a high index of refraction pathway between capillary and optical fiber using coupling gel. A straightforward ratio measurement, using a portion of the incident light as a reference, should suffice as a quantitative indication of refractive index. This is the first report of such a measurement. Our preliminary results include evaluation of both static an dynamic operating modes.

Static evaluation. Axial illumination refractive index measurements were made for air, methanol and ethanol, with the liquids being delivered to the flow cell with flow-rates of 10 μl/min. The measured signals for air, methanol and ethanol were 0.0, 0.71 and 0.90 V, respectively. Using the reference refractive index values of 1.000, 1.326 and 1.359 for these materials, we obained a response sensitivity of 0.38 RIU/V, where RIU = refractive index unit. Unfortunately, there was significant baseline noise, about ± 0.015 RIU, in the methanol and ethanol cases. The noise for methanol was slightly larger than for ethanol, an observation that we attribute to fluctuations in the degree of evaporative cooling at the capillary orifice. There were also long term variations, presumably due to mobile phase flow instabilities. Flow and temperature effects have been observed to influence the stability of "on column" refractive index detectors [23].

Dynamic evaluation. With a methanol mobile phase and reversed-phase column, injections of a methanol–toluene mixture, with a refractive index of 1.408, were made and the signal was recorded. A typical chart recording is shown in Fig. 11. The peak height was 0.06 RIU, which when added to 1.326 (methanol mobile phase) gives a measured value of 1.386. This is very reasonable, considering dilution on the column. The methanol–toluene peak represents detection close to the detection limit, due to significant baseline noise. Obviously, we are less confident in these results, relative to the fluorescence measurements. We observed degraded column performance and unstable electronics, both in the laser and the log ratio amplifier. The basic premise of a dynamic measurement, however, was supported, namely that a transient signal could be recorded accurately and reproducibly.

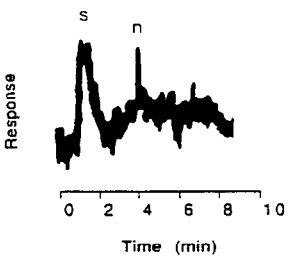

Fig. 11. Refractive index chromatogram. s = 80-nl injection of toluene–methanol with refractive index 1.408; n = electronic noise spike.

CONCLUSIONS

We have demonstrated the successful coupling of micro-LC with axial illumination fluorescence and refractive index detection. The promise of significantly enhanced concentration detectability was not realized in our studies, probably due to low mobile phase refractive index, low laser power (perylene fluorescence measurements), small area detector and, to a certain extent, nebulization noise. Higher mobile phase refractive index would have given more light interaction with the lumen and larger signals. Since the detector area determines the detected volume, a larger detector area (*e.g.* that for a 25-mm diameter photomultiplier) would have resulted in larger detected volume and higher signal levels. Less nebulization noise would have yielded higher signal to noise values, throughout. Effective nebulization of mobile phase at the 5 and 10 μl/min flow-rate levels was achieved with our flow cell. Despite these limitations, we have obtained reasonable results for *both* detection schemes.

The most significant noise sources appeared to be related to nebulization and eletronics. Two possible contributions include refractive index perturbations at the liquid orifice of the capillary during nebulization and microbending losses from a "vibrating" capillary. The Babington nebulization technique was very effective, especially in being easily miniaturized and immune from problems such as residue formation and significant cooling. Alternatives to this approach would not likely be as effec-

tive. Immobilizing the capillary in our flow cell was easily done, however some vibrations remained especially in the refractive index flow cell. Operating the device at elevated, constant temperature would have been helpful in minimizing drift and some spurious low frequency noise. Refinements in both optics and electronics are needed to realize optimum performance.

Axial illumination is a versatile technique for detection in miniaturized liquid chromatographic methods. The technique has been demonstrated for absorbance detection [2], fluorescence and refractive index measurements. Improvements in materials and fabrication techniques may result in more effective designs and higher performance. Technological advances in the area of integrated optical devices may serve as a model. An exciting possibility, whole column detection, using the axial illumination technique may be demonstrated in the near future.

ACKNOWLEDGEMENTS

We are grateful to Dr. Mack Harvey of Valco Instruments for the loan of the electric actuator for the microinjector. We also thank Mr. Kavin Morris of the TTU Chemistry machine shop for fabrication of the flow cell.

REFERENCES

1 I. H. Grant and W. Steuer, *J. Microcol. Sep.*, 2 (1990) 74–79.
2 X. Xi and E. S. Yeung, *Anal. Chem.*, 62 (1990) 1580–1585.
3 J. A. Taylor and E. S. Yeung, *J. Chromatogr.*, 550 (1991) 831–837.
4 X. Xi and E. S. Yeung, *Appl. Spectrosc.*, 45 (1991) 1199–1203.
5 J. V. Sweedler, J. B. Shear, H. A. Fishman, R. N. Zare and R. H. Scheller, *Anal. Chem.*, 63 (1991) 496–502.
6 K. Jinno and C. Fujimoto, *LC · GC*, 7 (1989) 328–338.
7 A. Abbas and D. C. Shelly, *47th Southwest Regional American Chemical Society Meeting, San Antonio, TX, Oct. 1991*, paper No. 38.
8 W. Lei, K. Fujiwara and K. Fuwa, *Anal. Chem.*, 55 (1983) 951–955.
9 P. Dasgupta, *Anal. Chem.*, 56 (1984) 1401–1403.
10 K. Tsunoda, A. Nomura, J. Yamada and S. Nishi, *Appl. Spectrosc.*, 43 (1989) 49–55.
11 K. Tsunoda, A. Nomura, J. Yamada and S. Nishi, *Appl. Spectrosc.*, 44 (1990) 163–165.
12 R. F. Browner and A. W. Boorn, *Anal. Chem.*, 56 (1984) 875A–888A.
13 T. J. Edkins and D. C. Shelly, *J. Chromatogr.*, 459 (1988) 109–118.
14 T. J. Edkins and D. C. Shelly, *Anal. Chim. Acta*, 246 (1991) 151–159.
15 M. C. Harvey and S. D. Stearns, *J. Chromatogr. Sci.*, 21 (1983) 473–477.
16 D. C. Shelly, V. L. Antonucci, T. J. Edkins and T. J. Dalton, *J. Chromatogr.*, 458 (1989) 267–279.
17 R. P. W. Scott, *Liquid Chromatography Detector (Journal of Chromatography Library*, Vol. 33), Elsevier, Amsterdam, 2nd ed., 1986, pp. 18 and 22.
18 L. S. Lee, *J. Am. Oil. Chem. Soc.*, 66 (1989) 1398–1409.
19 G. J. Diebold and R. N. Zare, *Science, (Washington, D.C.)*, 196 (1977) 1439–1441.
20 T. Panalaks and P. M. Scott, *J. Assoc. Off. Anal. Chem.*, 60 (1977) 583–589.
21 M. Manabe, T. Goto and S. Matsuura, *Agric. Biol. Chem.*, 42 (1978) 2003–2007.
22 S. B. Miller, in D. Marcuse (Editor), *Integrated Optics*, IEEE Press, New York, 1973, pp. 18–22.
23 A. E. Bruno, B. Krattiger, F. Maystre and H. M. Widmer, *Anal. Chem.*, 63 (1991) 2689–2697.